

## **MOTION CHARACTERISTICS OF THE NATIONAL ADVANCED DRIVING SIMULATOR**

Chris Schwarz, Tad Gates, Yiannis Papelis

National Advanced Driving Simulator

University of Iowa

2401 Oakdale Blvd

Iowa City, IA 52241

319-335-4642 (phone)

319-335-4658 (fax)

[cschwarz@nads-sc.uiowa.edu](mailto:cschwarz@nads-sc.uiowa.edu)

Submitted July 7, 2003

### **ABSTRACT**

The large excursion capabilities and redundant degrees of freedom of the National Advanced Driving Simulator (NADS) motion system provide unique control and tuning challenges. The multi-belt system that drives the crossbeam and the belt that drives the turntable are both innovations in simulator technology. This paper will present some of the characteristics of the motion system, paying particular attention to the capabilities unique to the NADS. Several measurements of the motion characteristics have been taken to help quantify the performance of the device. Specific measurements include transfer functions between command and feedback accelerations, noise at constant velocity, ½ hertz noise levels, and dynamic threshold measurements. The motion controller tuning approach is one that results in a moderate bandwidth, relatively low noise level, and good response for high amplitude inputs.

### **INTRODUCTION**

The National Advanced Driving Simulator (NADS) was built at the University of Iowa after a nationwide competitive process held by the federal DOT. The design of the NADS is geared for use by common drivers rather than by expert operators. As a result, every system in the simulator has the highest possible fidelity. The visuals wrap a complete 360 degrees around the cab. The dome is large enough to accommodate a complete cab of most passenger vehicles. The interiors of the cabs are completely realistic; and extraneous research and safety equipment is unobtrusive or hidden from the sight of the driver. An extensive set of audio cues is played through a dozen speakers both inside and outside of the cab. The motion system augments a standard Stewart platform with a large excursion X-Y system, a yaw turntable on top of the hexapod, and vertical vibration actuators in the dome, resulting in a nine degree-of-freedom (DOF) system with augmented bandwidth in the vertical direction.

The motion system is integral to providing a complete set of cues to the driver; and the use of a large motion theater means that maneuvers that could not be simulated in other devices without significant false cues can be done in the NADS. However, those same capabilities pose unique challenges to maintaining high levels of motion quality. This paper examines some of the characteristics of the motion system. These characteristics make evident tradeoffs that must be taken into account when tuning the motion controllers. The main tradeoff is between noise levels at low speeds and performance at high accelerations. Aggressive tuning of the controllers extends the bandwidth of the system response; but also tends to worsen the noise. This is true even for the hexapod, which is used in many simulators today. The approaches used by Grant [1,2] to quantify motion characteristics for the UTIAS and VIRTTEX simulators are largely followed here.

Several differences between the hexapod and the X-Y motion system deserve comment. The primary difference is the method of actuation. The hexapod is hydraulically actuated, while the X-Y system uses electric motors. Typically, hydraulically actuated motion is smoother than its electrical counterpart because of mechanical backlash in the motor gear reduction. On the other hand, large electric motors have a higher specific power than their hydraulic counterparts because of the volume of oil required to power a large system. Electromechanical and hydraulic machines exhibit imperfections unique to each type of device.

The main hydraulic imperfections include a resonance at the wavelength matching the oil column height in the actuator, and a turn-around nonlinearity that is seen as the valve transitions the oil flow from one path to another when the actuator changes direction. The main imperfection of the electromechanical system is caused by the gearboxes attached to each motor [3,4]. A second characteristic of the X-Y system is caused by the hydrostatic bearings that support the carriage and crossbeam on a cushion of hydraulic oil [5]. Friction and stick-slip, or stiction, exhibits itself both at turn-around and at low speeds. Unlike backlash, the effects of friction are speed dependent [5]. The chatter caused by stick-slip at low velocities will disappear at higher speeds. It can also be eliminated by stiffening the plant or the controller [6].

A second difference between the two systems is in their symmetry. The hexapod has tri-axial symmetry while the X-Y system has only uni-axial symmetry. Because of its higher degree of symmetry, the hexapod has fairly uniform motion characteristics for X and Y motion as well as for roll and pitch motion. As well, the tuning parameters for the aforementioned pairs are quite similar. In contrast, the X-Y system enjoys only uni-axial symmetry, although this it has on both the X and Y DOFs. The Y system is responsible only for moving the carriage that supports the hexapod and dome; while the X system must push the whole crossbeam that supports the carriage and weighs substantially more than the carriage, hexapod, and dome put together. Even though each belt/motor/gearbox unit in the X-Y system is identical, they are not evenly distributed between the two directions; thus, the responses vary somewhat. Accordingly, the tuning parameters are also unique for the X and Y directions. This situation makes it more difficult to mix the X and the Y motion in some cases. For example, when using the X-Y diagonal for on-center driving, the different turn-around bumps in the two directions may combine to form a 'diagonal' bump that can be disconcerting to the driver.

A third difference between the two systems has already been touched upon; and that is the size difference. The hexapod actuates about 12 tons, while the X-Y system has to move up to 88 tons. The main consequence of this fact is that the X-Y system has to be over-actuated, i.e., several actuators applied to each DOF. The control strategies that result from this are described in more detail in the body of the paper.

It was not assumed a priori whether the X-Y system would be more susceptible to the effects of backlash or stiction or some other effect. In the sequel, we study several test results and relate them back to the set of probable causes described above. The tests were conducted at a time when some repairs were ongoing. As a result, a pair of motors at one end of the southern-most belt (negative Y quadrants) was turned off. This fact is not expected to alter any of the conclusions reached; however, it will certainly have some effect on the data. This will be noted, as deemed necessary, throughout the presentation of results.

The first section of the paper describes in some detail the control strategies employed on the motion system. This is followed by a section on the transfer functions of the X-Y system and turntable. The next section reports DC noise results obtained from driving the X-Y system at constant velocities. The noise levels at ½ Hz sinusoidal inputs are reported next, followed by results on the dynamic threshold.

## **MOTION CONTROL AND TUNING**

### **Motion Actuators**

The most familiar component of the NADS motion platform is the six DOF Stewart platform, which has six hydraulic actuators with 36.5" of stroke. The actuators can deliver a maximum of 16,500 lbs of force per actuator yielding a peak of 1.0g on the vertical axis. The Stewart platform has been enhanced by adding a turntable allowing the dome to rotate 330 degrees in either direction. The turntable rests on a large axial/radial bearing and can be rotated by a serpentine Kevlar belt and three hydraulic servo motors with gear reducers. The system is constructed to reduce belt slippage and reduce any flex in the belt itself. On top of the motion platform, inside the dome, are four hydraulic vibration actuators. These actuators provide 0.4 inches of dynamic stroke. The actuator is constructed with a built-in reaction mass to mitigate the vibration passed into other components attached to the platform. A unique feature of the NADS is that the Stewart platform is mounted on a large, 64 by 64 foot, two DOF motion system. The X-Y system is comprised of 28 100 hp electric motors and variable frequency drives. The motor assemblies are divided into groups of four, each group driving a single belt in the system. Six belts are evenly spaced and attached to the crossbeam for the X axis, while one belt is used to drive Y axis carriage that supports the Stewart

platform. Each belt is constructed of stainless steel and is fixed to the attachment point on the crossbeam or carriage with load pins. The total mass of the crossbeam assembly, Stewart platform, display system, and cab is approximately 176,000 lbs.

### **Control Strategies**

High-level motion apportionment is straightforward. Low frequency translational acceleration commands are sent to the large excursion X-Y system, while higher frequency commands are sent to the hexapod. The cutoff frequency is adjustable by the user. Vertical accelerations, along with roll and pitch rotational velocities, are sent solely to the hexapod. Yaw rotational motions are apportioned completely to the turntable.

The mass of the simulator is great enough that multiple actuators are required to obtain adequate response in several directions. As a result, control strategies must be employed that resolve issues of over-constrained actuation, which can cause fighting between actuators and unwanted vibration. The control strategies for the hexapod are similar to those at VIRTTEX [1] and discussed in more detail by MTS [7]. Since the hexapod uses six actuators to realize six degrees of freedom, it is properly constrained. In contrast, the other degrees of freedom are over-constrained by multiple actuators. The yaw turntable is driven by three hydraulic motors, the Y system by four electric motors, and the X system by 24 electric motors.

There are two motor/gearbox sets mounted at each end of each belt. The pair is attached to a common shaft on which is installed a larger diameter drum, and the belt wrapped around this drum at each end. Each motor is controlled by a local variable frequency drive (VFD). One of the motors on a shaft can be configured to be a master, and the other to be a slave; and the VFDs have parameters that affect how tightly coupled the two motors are. Therefore, only one control signal is required per motor pair; and local motor control parameters can be tuned to optimize motor cooperation. Likewise, the same control signal is used to command opposite ends of each belt. Unlike the motor pair on a common shaft, there is no local cooperation between motors on different shafts. Rather, minor differences in motor/gearbox performance on different ends of a belt are absorbed by the tension compliance of the belt itself, which has a nominal (resting) tension of around 30,000 lbf. Thus, each belt, with the motors that drive it, can be considered as a cooperative actuating system.

Treating each belt as an actuator, the Y system is no longer over-constrained. The X crossbeam, however, is still driven by six belts. The control strategy is to use these six actuators to control multiple modes of the crossbeam. Three position sensors are placed along the X crossbeam, one in the center and one on each end. These three sensors enable measurement of the amount of translation, yaw, and bend of the crossbeam. Each of these three modes has an independently tunable controller. The presence of additional force balancing servo loops in the crossbeam controller implicitly zeros out additional modes, allowing the X crossbeam control system to function properly. Similarly, the turntable's three actuators are made to cooperate with each other by the use of three force servo loops. These control loops can be tuned to control how tightly synchronized the turntable motors are.

All of the DOF controllers act on position, velocity, and acceleration error signals; thus, they are termed three variable controllers (TVCs). This arrangement effectively allows the engineer to tune the low, mid, and high frequency bands of the closed loop system. If a sensor signal is not available for any of the three feedback variables, it is calculated from the available signals. Given the large number of tuning parameters available for each motion DOF, it is possible to tune the system to optimize specific aspects of its operation. Usually, this is to the detriment of another aspect. For example, aggressive tuning that improves frequency response also increases the noise. Decreasing the noise, not only reduces the frequency response, but it can also reduce maximum achieved acceleration. Since delivery of the system, much work has been done to determine a tuning point that provides the best compromise possible, given the types of tasks necessary for the various research projects. To this point, an acceptable compromise for all DOFs except the yaw turntable has been reached. The turntable will be focused on in upcoming work.

The hexapod controller makes use of high fidelity feed-forward controllers that model the inverse hydraulics and the inverse payload [7]. These feed-forward blocks allow more precise open loop control of

the hexapod, thereby allowing the feedback controllers to be tuned more softly. The payload mass is about 22,000 lb which includes the mass of the cab inside the dome. Technically, the mass would have to be adjusted when cabs are changed out; but the constant is taken to be an adequate approximation over the range of dome payloads. Hexapod specific results are not presented in this paper, in order to allow more complete coverage of the novel aspects of the motion system.

## TRANSFER FUNCTIONS

The transfer functions of each DOF were identified by applying 25 Hz band-limited white noise to each DOF in turn. The translational DOFs were driven with a 0.03G amplitude signal, while the rotational DOFs were driven with a 6 deg/sec<sup>2</sup> amplitude signals. Non-driven channels were also recorded so that crosstalk between DOFs could be evaluated. Each test generated 90 seconds of data sampled at 500 Hz. The transfer functions were estimated using Matlab's transfer function estimator (TFE) in the signal processing toolbox [8], which uses Welch's modified periodogram method, and calculates the ratio of the cross spectral density to the power spectral density (PSD). A segment length of 7.5 seconds, or 3750 samples, was used with a Hanning window and 50% overlap. The frequency resolution using these numbers is about 0.13 Hz. Transfer function results for the X crossbeam and turntable are presented in this section. NADS system specifications call for less than 3dB variation in the magnitude response, and less than 30 degrees of phase lag up to 3Hz [9].

### X Crossbeam

The X Crossbeam transfer function was recorded at three different positions of the Y Carriage on the beam, specifically at -300 inches, zero inches, and 300 inches. This allows the cross talk between translational motion and the beam yaw and bend to be more completely characterized in the X-Y system's domain of operation. The three transfer functions between commanded and feedback X translational motion are shown in Figure 1.

X Crossbeam controller tuning is performed with the Y position at zero inches; thus, the corresponding transfer function has the flattest response of the three. The response with the dome at a Y position of -300 inches shows a resonance at 6.5 Hz, while the one at 300 inches has a more gentle resonance at 5 Hz. The three responses highlight the difficulty of tuning the crossbeam for operation throughout the whole room. If one tries to bring up the suppressed response of the center curve between 6 and 7.5 Hz, the resonance of the end curves would become worse. On the other hand, if one tries to extend the responses of the end curves beyond 7 or 8 Hz, one would worsen the resonance in the center curve. All three responses meet the 3dB and 30 degree lag conditions in the NADS specifications. It is appropriate to focus on the response in the center at the expense of the ends, since the percentage of time spent in the center of the beam is much greater than that spent near the limits of the motion.

The transfer function at the negative Y position is definitely affected by the missing pair of motors on the end belt. Ideally, the response would be closer to the one at the other end of the beam. It is still a fact, however, that variations in response do occur as the dome moves back and forth. A real-time adaptive controller was considered during NADS development but was rejected because of the added phase lag it would have introduced. It may be feasible, however, to use an adaptive controller to identify optimal tuning parameters in different positions, and then implement a continuous parameter scheduling approach to keep the closed loop response flat as the dome moves around the room.

The responses of the X Crossbeam yaw in the three positions along the beam are fairly consistent (see Figure 2); although one can see that the coherence at 300 inches is somewhat degraded. The low coherence of all three cases calls into question the accuracy of the transfer functions; however, it also indicates the weakness of the crosstalk. The main difference between the center and the ends is that there is a significant phase lead in the yaw response at the beam ends. The reason for this could be the presence of linear, feed-forward, gain scheduling in the crossbeam commands that is a function of the Y position of the dome along the beam, and which tries to compensate for the mass of the carriage and dome. Additionally, a slight resonance is visible just above 6 Hz. From experience, the maneuvers that excite this resonance are abrupt accelerations or decelerations with the dome near the limit of Y travel.

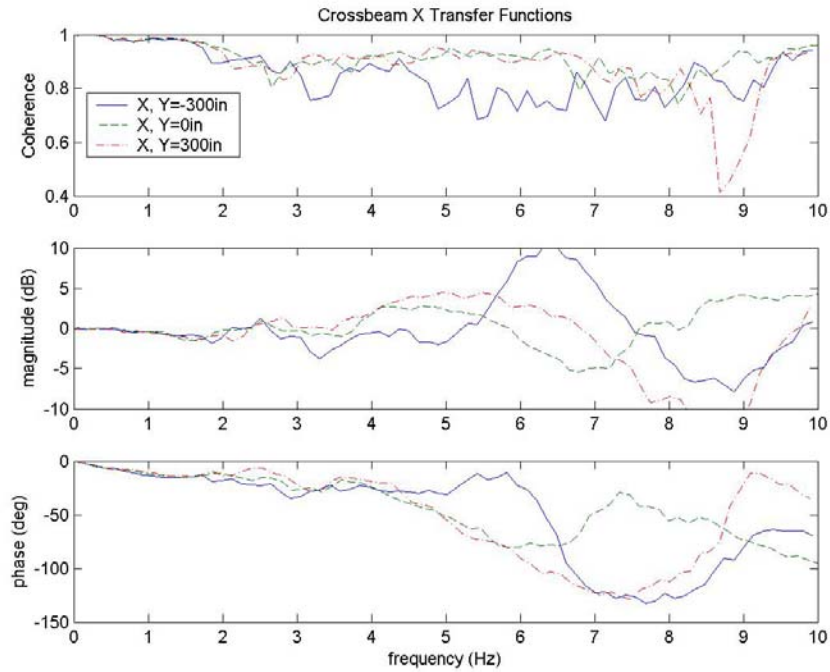


**Figure 1 Crossbeam X Transfer Functions at Three Y Positions**

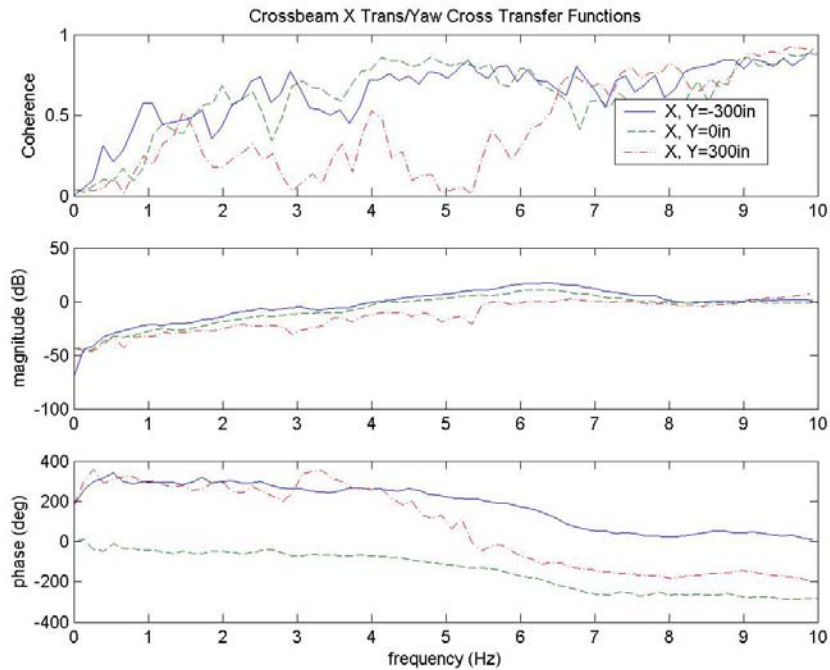


**Figure 2 Crossbeam X Trans/Yaw Cross Transfer Functions**

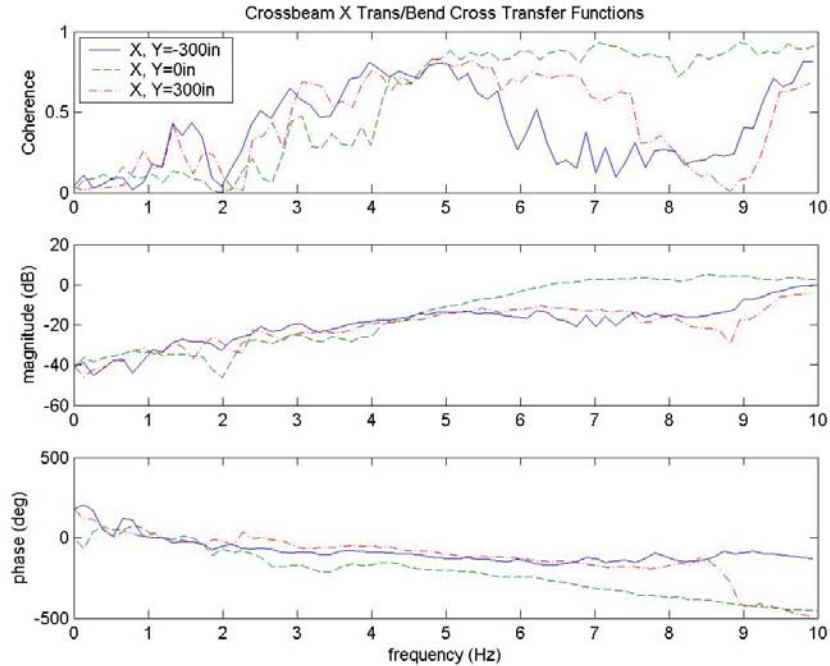


**Figure 3 Crossbeam X Trans/Bend Cross Transfer Functions**

The crosstalk transfer functions from the Crossbeam X and Crossbeam bend are shown in Figure 3. The bend mode is excited more when the dome is in the center of the beam; and this is evidenced by the higher magnitude of the center curve above 5 Hz. The bend mode is very lightly controlled and the yaw mode slightly more so. If too much authority is given to the bend controller, it interferes with the other modes. Likewise, if too much authority is given to the yaw controller, it interferes with the translational motion. Both the Crossbeam X yaw and bend accelerations are measured in the same unit as the crossbeam translational acceleration, since those modes are simple functions of the three position sensor readings along the beam. Because of this method of yaw and bend estimation, the crosstalk transfer functions are dimensionless, just like the driven transfer function.

**Yaw Turntable**

The yaw turntable is moved by a large belt that winds its way around three hydraulic motors, six idlers, and is wrapped around the turntable itself. Force balancing controllers operate to keep the three motors in full cooperation, and reduce problems associated with over constrained actuation. Even though the belt is tensioned, it is not rigid and not as stiff as the steel belts, so its response is not expected to have as high a bandwidth as the other DOFs. The turntable transfer function is shown in Figure 4. The -3dB point is at around 3 Hz, but the phase lag is quite large even by then; and there is a resonance that exceeds +3dB at around 1.2 Hz. It is possible to extend the response, and reduce the phase lag a little; but it tends to aggravate the resonance and cause instability at higher turntable velocities. The tuning of the turntable to its optimal performance is an ongoing effort. The cross transfer function between turntable yaw and hexapod yaw is shown to be reasonably small in Figure 5.

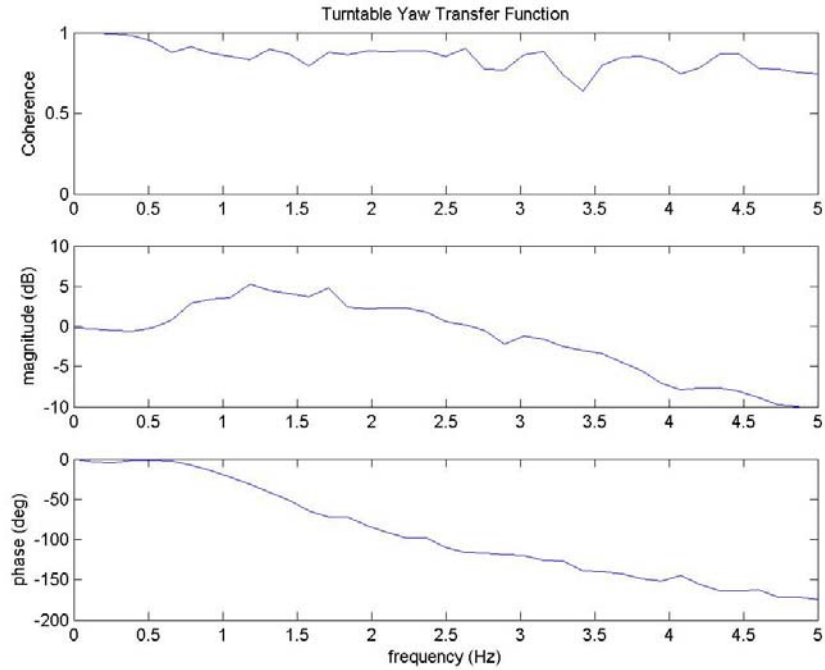


**Figure 4 Turntable Yaw Transfer Function**

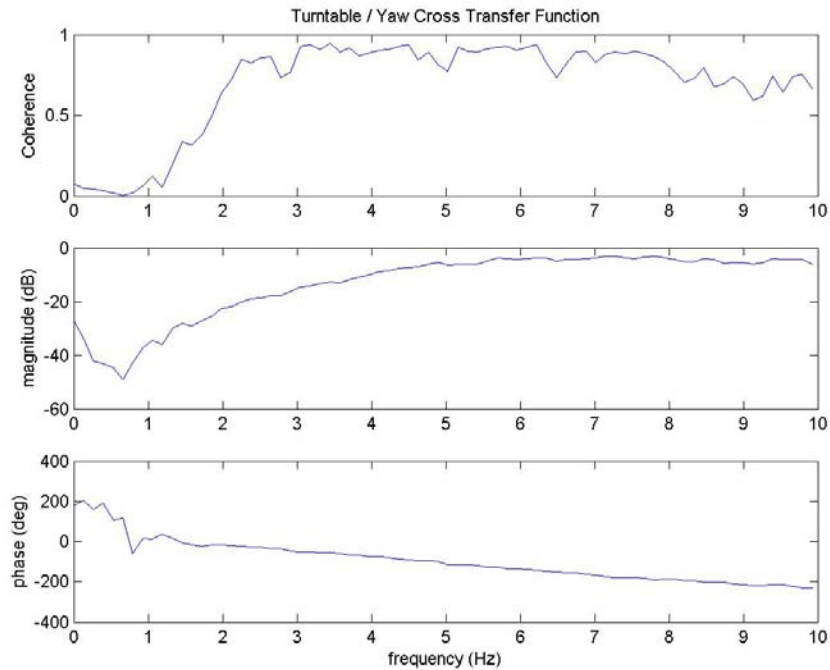


**Figure 5 Turntable/Hexapod Yaw Cross Transfer Function**

### DC NOISE

The X-Y motion system exhibits a certain amount roughness while traveling at constant velocities. The original specifications for the NADS allows up to 10mG RMS of noise per axis, and up to 20mG of noise during multiple axis motion [9]. A summary of vibration statistics during travel at 4 in/sec is given in

Table 1 below. The PSD of the acceleration error signal offers a picture of the frequency content of the vibration and it is shown in Figure 6. Notice that the peak at 2Hz is more pronounced on the Y Carriage, while the X Crossbeam PSD is flatter and more spread out. In this case, the use of multiple belts is helpful to reduce undesirable peaks by averaging noise from multiple sources. While the noise is within specifications, it is clear that the RMS value doesn't tell the whole story, and attention should also be paid to the maximum peak.

**Table 1. Vibration During Travel at 4 in/sec**

	X Crossbeam	Y Carriage
<b>RMS (mG)</b>	10	9
<b>90<sup>th</sup> %-ile (mG)</b>	17	15
<b>Max Peak (mG)</b>	40	36

The vibration experienced at 4 in/sec is the worst case. Another set of measurements taken during travel at 20 in/sec is presented in Table 2 below. The 20 in/sec value is the target velocity during preposition and docking motions; however, the vibration amplitude reported Table 1 is evident as the velocity ramps through 4 in/sec. These noise characteristics can be affected by tuning the motor control loops in the VFDs, and the VFD parameters currently in use attempt to balance roughness at low speed with acceleration performance.

The velocity dependence of the vibration points to stick-slip as being the most probable cause. The vibration is most likely a composite effect from several sources though. A second possible cause is a nominal amount of fighting that occurs between the two motors on each shaft, and which can only be reduced, not eliminated. This component is not speed dependent; and prevents the phenomenon from disappearing completely at higher velocities.

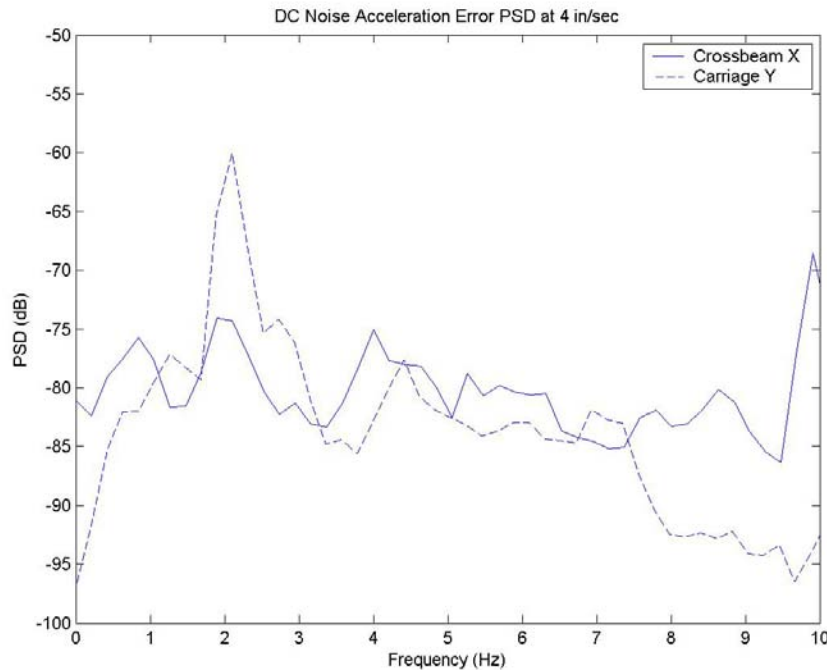


**Figure 6 Acceleration Error PSD During Travel at 4 in/sec**

**Table 2. Vibration During Travel at 20 in/sec**

	<b>Crossbeam X</b>	<b>Carriage Y</b>
<b>RMS (mG)</b>	7.5	6
<b>90<sup>th</sup> %-ile (mG)</b>	12	10
<b>Max Peak (mG)</b>	28	21

### HALF HERTZ NOISE

The variance of the feedback noise during the ½ Hz tests is estimated from the PSD of the noise. Using the PSD in this way allows the noise to be broken into different frequency components. Define the noise component of a particular frequency sample as

$$\sigma^2(k) = \frac{2}{N} P_{xx}(k\Delta f), \quad (1.1)$$

where  $P_{xx}$  denotes the PSD. Then the variance of a zero mean, WSS signal may be obtained from a one-sided PSD through the inverse DFT [10] evaluated at zero frequency [11]. This is expressed in terms of Equation (1.1) as

$$\sigma^2 = \sum_{k=1}^{N/2} \sigma^2(k). \quad (1.2)$$

Equations (1.1) and (1.2) are identical to the formulation presented by Grant [1] if a boxcar window is used. Now, different frequency components of the noise may be identified by extracting specific elements from the sum. Define the index,  $k_d$ , that picks the driven frequency, ½ Hz. Then the noise components at the driven frequency, low frequency harmonics, and high frequency harmonics are obtained by summing  $\sigma^2(k)$  over the index sets  $\{k_d\}$ ,  $\{2k_d, 3k_d\}$ , and  $\{4k_d, 5k_d, \dots, \lfloor N/2\Delta f \rfloor\}$  and denoted by  $\sigma_d^2$ ,  $\sigma_{lf}^2$ , and  $\sigma_{hf}^2$  respectively. The total noise of the acceleration error is estimated by subtracting the noise at the driven frequency from the overall feedback signal variance as

$$\sigma_{tot}^2 = \sigma^2 - \sigma_d^2. \quad (1.3)$$

That portion of the noise that can be thought of as ‘roughness’ is defined by subtracting the low frequency harmonics from the total noise as

$$\sigma_r^2 = \sigma_{tot}^2 - \sigma_{lf}^2. \quad (1.4)$$

The ½ Hz noise tests were performed by recording 90 seconds of data at each amplitude in a series of six increasing amplitudes. Every channel of recorded data was sampled at 200 Hz. The PSD was implemented using Matlab’s PSD command, which uses Welch’s periodogram averaging method. Boxcar windowing is used on segments of 10,000 samples (or 50 seconds), with 50% overlap between segments. The resulting resolution in the frequency domain is 0.02 Hz.

### X Crossbeam

The noise characteristics of the X Crossbeam were measured by applying sinusoidal acceleration commands of varying amplitude and ½ Hz frequency and recording the feedback acceleration. The amplitudes applied were 0.01G, 0.02G, 0.04G, 0.07G, 0.10G, and 0.13G; and the command and feedback signals for two wavelengths are plotted in Figure 7.

The noise appears to be dominated by the same kind of roughness that was observed in the DC noise tests reported earlier. There are two main types of nonlinearities that contribute to the turn-around bump in the X-Y system. First, there is backlash from the gearbox on each motor; and second, there is stiction associated with the hydraulic bearings on which the crossbeam and carriage float. Generally, the effects of stiction can be observed just before the acceleration peaks, while backlash can be seen just after the peaks [4]. Even knowing this, the effects of one or the other are not always discernable from among the noise.

It turns out that the turn-around bump may be clearly perceived by the driver even if it is not distinctly visible in the acceleration feedback signals. Tests done with human drivers indicate that the X turn-around bump is much less discernable than the Y turn-around bump, even though the Y acceleration signals don't show the effects of backlash or stiction any more than the X signals do. It would be expected that one could separate the effects of backlash and stiction from the noise in post processing; however, a real-time method would have to be integrated into the motion software in order to extend the benefits of signal processing to the tuning process.

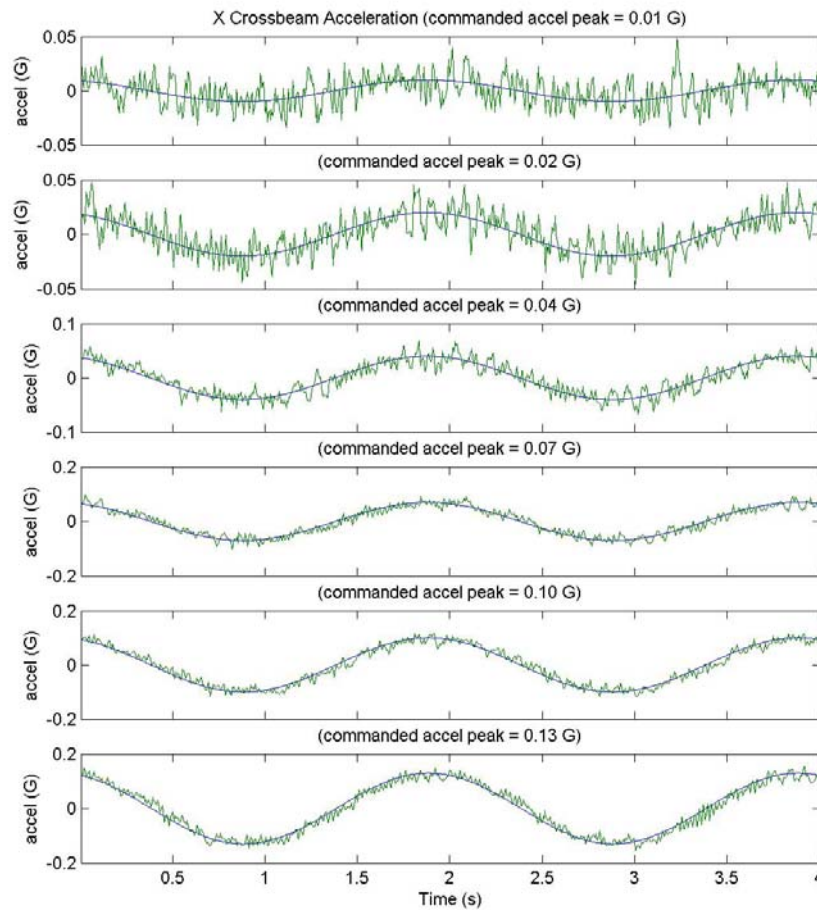


**Figure 7 Crossbeam X Half Hertz Noise Time Histories**

A simple example of potentially helpful post-processing is to average the acceleration signals for every period (there are about 40 useful periods of data in 90 seconds). Ideally, random noise will be averaged out, while predictable effects, such as stiction and backlash, will be reinforced. This was done for the X Crossbeam; and the results are shown in Figure 8. Observe that the desired reinforcement is evident just after both acceleration peaks. Due to their location, these effects are attributed to backlash. The distortions

in the acceleration signals just before the peaks are not considered a real effect because they change sign from one curve to the next, and they are not uniformly present in both directions.

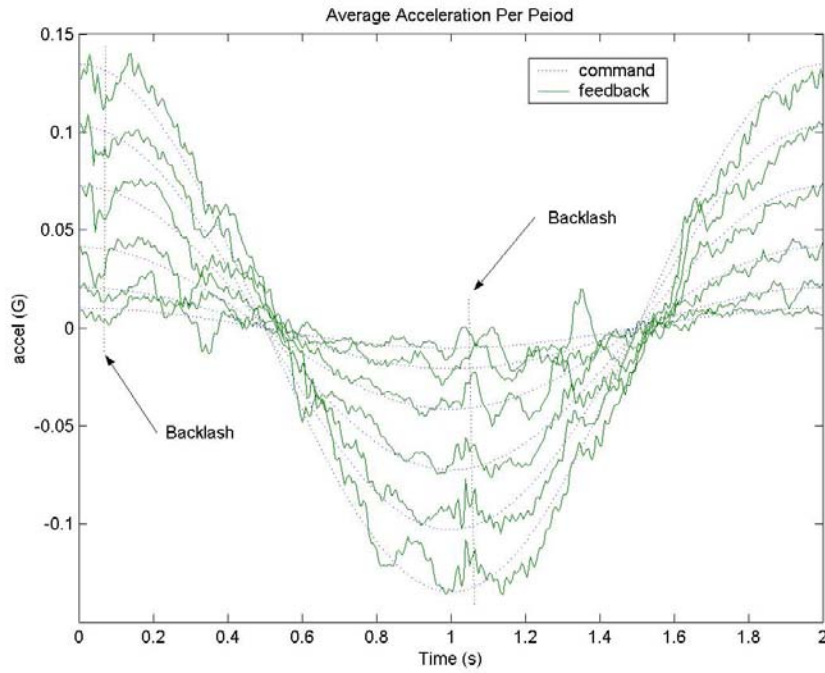


Figure 8 Crossbeam X Half Hertz Average Acceleration Per Period

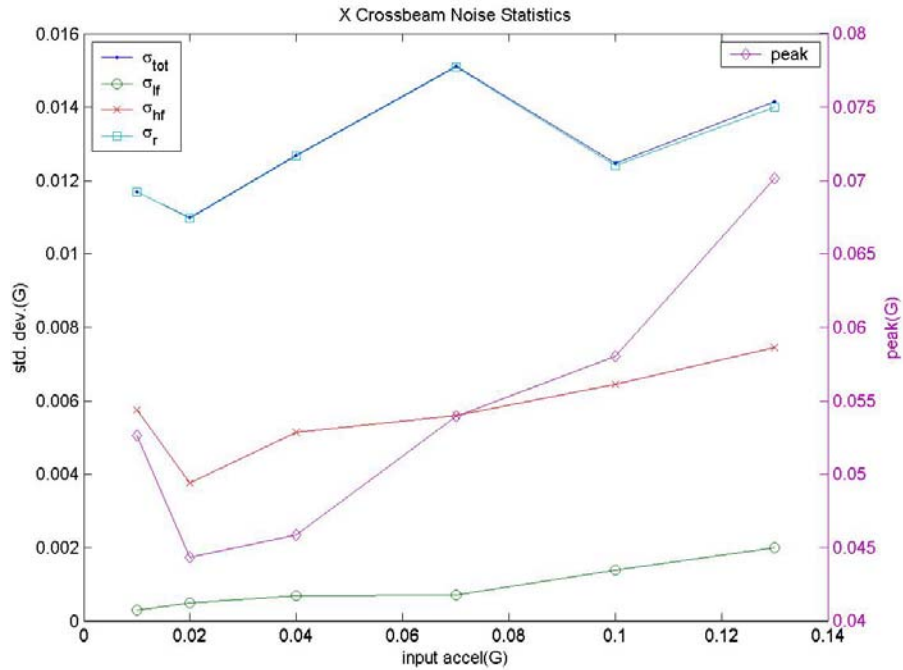


Figure 9 Crossbeam X Half Hertz Noise Statistics

It is evident from the noise statistics shown in Figure 9 that roughness dominates the noise at all applied amplitudes, and that the average standard deviation of that roughness is around 13 mG. The peak noise drops from the first to the second amplitude, and then rises monotonically for the rest of the amplitudes in the series. Recalling that the DC noise is larger at 4 in/sec than at 20 in/sec, it is likely that the same behavior is being observed here. A certain degree of roughness is inherent in the use of electric motors as actuators; and by coupling two of them to a common shaft.

### Yaw Turntable

The set of amplitudes applied to the yaw turntable were chosen to be 1 deg/sec<sup>2</sup>, 2 deg/sec<sup>2</sup>, 4 deg/sec<sup>2</sup>, 6 deg/sec<sup>2</sup>, 8 deg/sec<sup>2</sup>, and 10 deg/sec<sup>2</sup>. The turntable has noise characteristics that are unique with respect to the rest of the motion system, due to the nature of the turntable actuation. The resonance between 1 and 1.5 Hz in the turntable transfer function is evident in the ½ Hz noise plots in Figure 10. The tradeoff between response and noise performance is most pronounced here. A tuning which effectively suppresses the resonance will also reduce the bandwidth somewhat; but it may also eliminate the response of the smallest amplitude input. The observed effect, in that case, is like a deadband in the belt; and it is likely that there is some free play in the belt, which is only overcome with an aggressive tuning of the controller. Because of the visible resonance, the averaging process used on the X Crossbeam does not work nearly as well on the turntable.

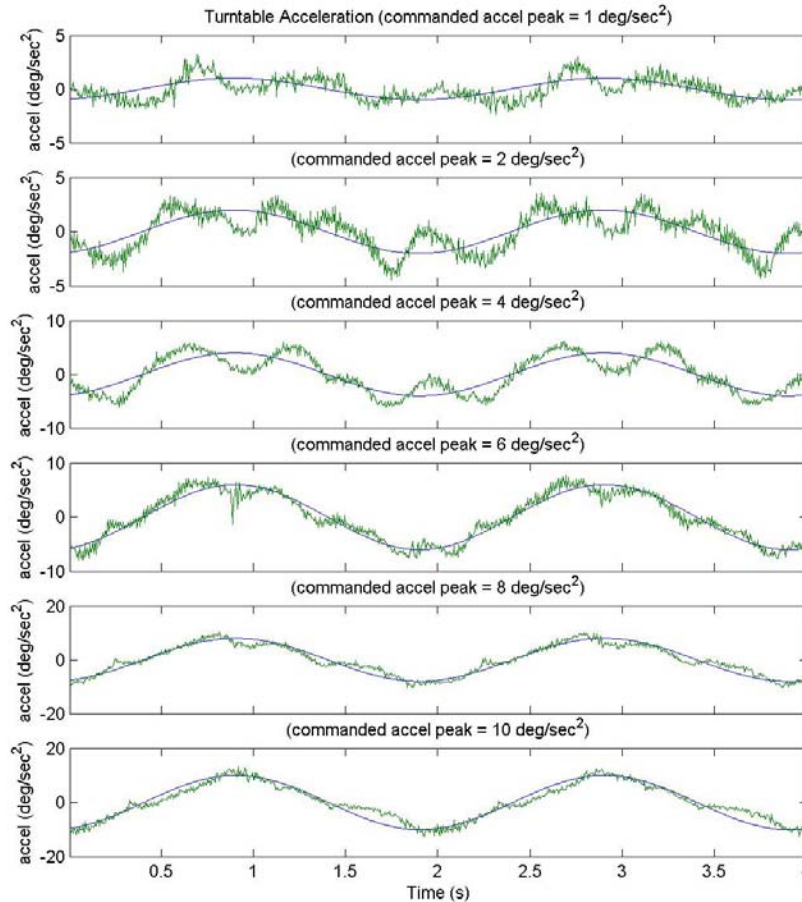


Figure 10 Turntable Half Hertz Noise Time Histories

Some interesting effects are observed in the turntable noise statistics shown in Figure 11. The low frequency noise is the largest component for the third and sixth amplitudes in the series. This can be directly attributed to the low frequency turntable resonance. It is interesting to note that the low frequency noise component drops dramatically from the third to the fourth amplitudes in the series; and this is easily confirmed by observing the time histories in Figure 10 as well. Amplitude dependence is a hallmark of many nonlinear systems; and this tuning works as well as it does precisely because the resonance that is observed for inputs less than 6 deg/sec<sup>2</sup> is somewhat mitigated for larger inputs, which are common in driving scenarios with turns.

The peak noise drops from the fourth to the fifth amplitudes in the series. The large peak is easily observed in the fourth time history in Figure 10, and it appears to be caused by turn-around bump because of its location and its sharpness. Some turn-around bump is expected from valve effects in the hydraulic motors; but coordination between the three motors is also expected to spread out the bumps as was seen in the X-Y system. The observed turn-around bumps are less sharp in the fifth time history and almost non-existent in the last one.

A unidirectional phenomenon is evident in the last two subplots of Figure 10 just before the negative acceleration peaks. It is consistent with velocity dependent stiction in the belt; but it is not nearly as noticeable in the other direction.

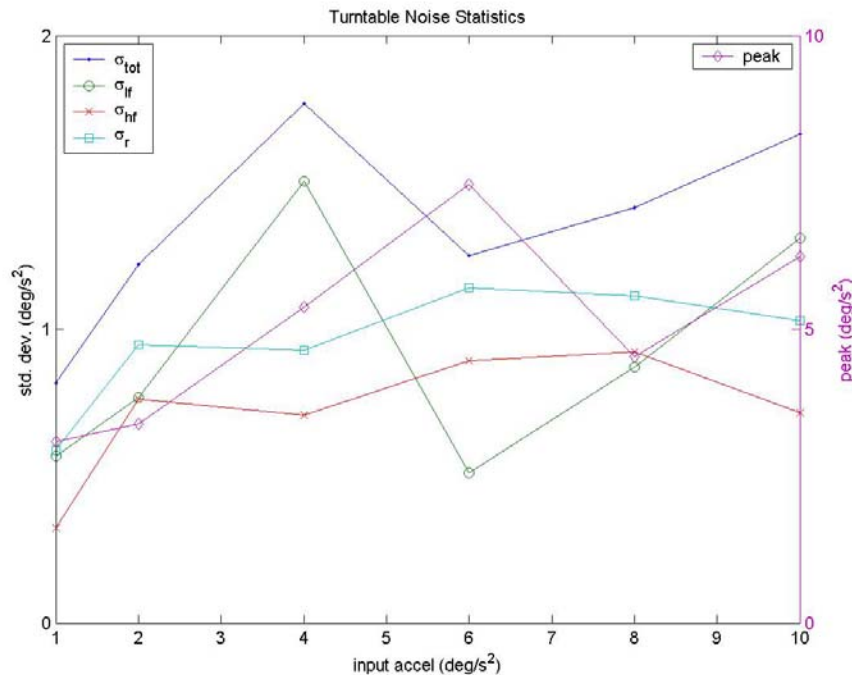
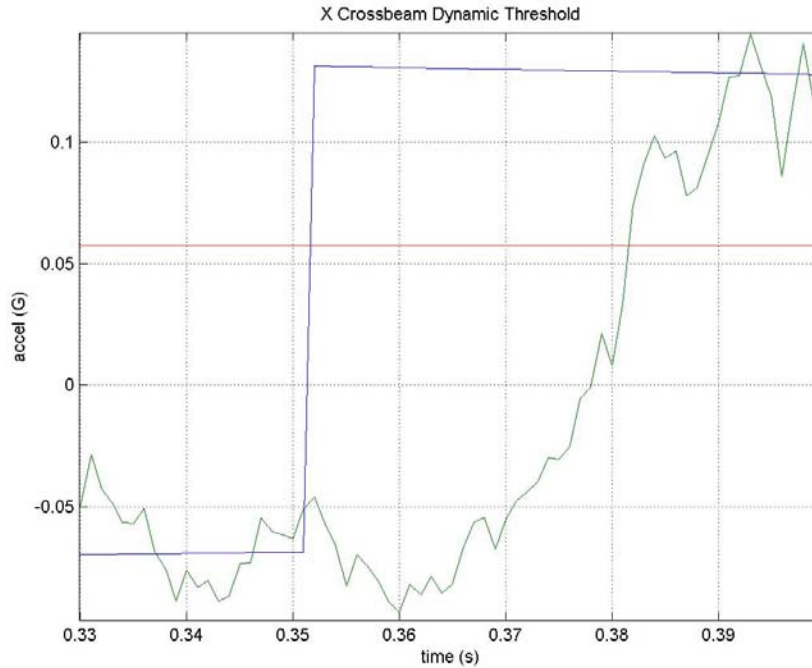


Figure 11 Turntable Half Hertz Noise Statistics

### DYNAMIC THRESHOLD

The dynamic threshold is a measure of latency in the motion system. It is measured by applying a square wave to the DOF under test and measuring the time to achieve 63% of the commanded value. Additionally, the time it takes for the response to begin after the command steps is called the deadtime. A 0.2G peak-to-peak square wave was applied to the X Crossbeam and Y Carriage; and a 20 deg/sec<sup>2</sup> peak-to-peak square wave was applied to the turntable. An ideal square wave was not obtained due to filtering present in the motion software; however, the distortion is not large on the time scale of the latency. Figure 12 shows the dynamic threshold for the X Crossbeam. The solid horizontal line that crosses the command and feedback curves marks off 63% of the commanded step.

Table 3 summarizes the dynamic threshold for the X Crossbeam, Y Carriage, and turntable DOFs. Generally, the lower the bandwidth of the closed loop system, the longer the dynamic threshold will be. This is why the turntable latency is so much larger than the crossbeam. The difference in latency between the X and Y axes probably indicate that the controller tunings are not quite the same. Dynamic threshold has not heretofore been used as a measure of performance of the controller tunings; and it may be helpful to utilize this measure to further synchronize the X and Y responses.



**Figure 12 Crossbeam X Dynamic Threshold Measurement**

**Table 3. Dynamic Threshold Estimates for X, Y, and Turntable**

	<b>Amplitude (p-p)</b>	<b>Deadtime (ms)</b>	<b>Threshold (ms)</b>
<b>X Crossbeam</b>	0.2 G	20	30
<b>Y Carriage</b>	0.2 G	30	45
<b>Turntable</b>	20 deg/s <sup>2</sup>	60	90

## CONCLUSIONS

We have examined several characteristics of the NADS motion system, focusing specifically on the large excursion X-Y system and the yaw turntable. Each of these systems exhibits unique effects that impact overall motion performance. The electromechanical actuators used in the X-Y system suffer from input backlash, which is perceived by the operator as a turn-around bump. Stiction is observed during low velocity motion due to the hydrostatic bearings that support the heaviest pieces of the motion base. Over-constrained actuation is required on multiple DOFs by the size of the motion base. As a result, there is a certain amount of noise caused by imperfect cooperation between adjacent actuators. Bandwidth and dynamic threshold were seen to vary among the various motion sub-systems. The ordering of motion

system components by bandwidth, from lowest to highest, is given by the following: yaw turntable, X-Y system, hexapod, and vibration actuators.

An intelligent utilization of the motion system requires an understanding of its operation, even at the lowest level. For example, effective strategies for reducing the turn-around bump, based on the results reported here, include apportioning more of the motion to the hexapod, and using the X Crossbeam for the most sensitive direction, since it smoothes out the bump through averaging over the belts. The observed characteristics also can result in recommendations for system modifications. For example, an adaptive identification scheme may aid in keeping the transfer functions of the X-Y system flat throughout their domains of operation. In addition, the bandwidth dividing approach that is used between the X-Y system and hexapod might be fruitfully applied between the turntable and hexapod as well. Perhaps most useful from a maintenance standpoint, regular monitoring of the simulator motion characteristics using the tests described here can help to pinpoint and diagnose degradation in the motion performance over time.

## REFERENCES

1. Grant, P., Artz, B., Greenberg, J., Cathey, L. Motion Characteristics of the VIRTTEX Motion System. Proceedings of the 1<sup>st</sup> Human-Centered Transportation Simulation Conference. Iowa City, IA, 2001.
2. Grant, P. Motion Characteristics of the UTIAS Flight Research Simulator Motion-Base. UTIAS Technical Note No. 261, July, 1986.
3. Boneh, R., Yaniv, O. Reduction of Limit Cycle Amplitude in the Presence of Backlash. Journal of Dynamic Systems, Measurement, and Control. Vol 121, No. 2, pp. 278-284, 1999.
4. Ezal, K., Kokotovic, P.V., Tao, G. Optimal Control of Tracking Systems with Backlash and Flexibility. Proceedings of the 36<sup>th</sup> IEEE CDC, SanDiego, CA, Dec. 1997, pp. 1749-1754.
5. Armstrong-Helouvry, B., Dupont, P., De Wit, C.C. A Survey of Models, Analysis Tools and Compensation Methods for the Control of Machines with Friction. Automatica, Vol. 30, No. 7, Section 2.1, pp. 1084-1090, 1994
6. Armstrong-Helouvry, B., Dupont, P., De Wit, C.C. A Survey of Models, Analysis Tools and Compensation Methods for the Control of Machines with Friction. Automatica, Vol. 30, No. 7, Section 4.3.1, pp. 1115-1116, 1994
7. Carmein, J.A., Clark, A.J. New Methods for Increased Fidelity and Safety of Simulation Motion Platforms. AIAA Modeling and Simulation Technologies Conference. Boston, MA, 1998, pp. 295-304.
8. The Mathworks. Signal Processing Toolbox Users Guide, The Mathworks Inc., Version 5, September 2000.
9. System Development Specification for the NADS. NADS SDS.002 REV B, TRW, November 2000.
10. Kamen, E.W., Heck, B.S. Fundamentals of Signals and Systems Using Matlab. Prentice Hall, 1997, pp. 278.
11. Vaidyanathan, P.P. Multirate Systems and Filter Banks. Prentice Hall, 1993, Appendix B.